Clays and Clay Minerals, Vol. 37, No. 3, 211–218, 1989.

EFFECTS OF OCTAHEDRAL-IRON REDUCTION AND SWELLING PRESSURE ON INTERLAYER DISTANCES IN Na-NONTRONITE[1]

JUN WU,[2] P. F. LOW, AND C. B. ROTH
Department of Agronomy, Purdue University
West Lafayette, Indiana 47907

Abstract—A new type of environmental chamber for X-ray diffraction was designed that could sustain elevated, internal pressures of nitrogen or any other gas under oxygen-free conditions and that allowed the positions of the specimen and edge aperture to be adjusted by remote control. It was used to determine the values of the interlayer spacing, λ, of nontronite from Garfield, Washington, in different stages of reduction at different values of Π, the swelling pressure of the nontronite. At equilibrium, Π was equal to the pressure under which water was expressed from the clay. Both partially and fully expanded layers were found to exist in the reduced nontronite, the fraction of partially expanded layers increasing with increasing Π and Fe^{2+}/Fe^{3+}, the ratio of Fe^{2+} to Fe^{3+} in octahedral sites. Also, λ for the partially expanded layers was found to depend on Fe^{2+}/Fe^{3+} but not on Π, and λ for the fully expanded layers was found to depend on Π but not on Fe^{2+}/Fe^{3+}. These findings were interpreted to mean that the reduction of Fe affected the short-range interlayer forces, but not the long-range ones.

Key Words—Interlayer distance, Iron, Nontronite, Reduction, Swelling pressure, X-ray powder diffraction.

INTRODUCTION

In her work on the swelling of montmorillonites, Foster (1953) observed that a blue-gray (reduced) sample of Wyoming bentonite swelled less than an olive-green (oxidized) sample. This observation and the observation that the swelling of a clay is related to the *b* dimension of its unit cell (Ravina and Low, 1972, 1977), which depends on the oxidation state of the octahedral Fe (Kohyama *et al.*, 1973), prompted Stucki *et al.* (1984c) to study the effect of the oxidation state of octahedral Fe on the swelling of smectites. They found that the swelling of these clays decreased as the reduction of octahedral Fe increased. Inasmuch as unexpanded, partially expanded and fully expanded clay layers can coexist in the same system (Foster *et al.*, 1955; Rhoades *et al.*, 1969; Viani *et al.*, 1983, 1985), this decrease in swelling on reduction could have been caused by the conversion of fully expanded layers to unexpanded or partially expanded layers or by a decrease in the distance between fully expanded layers. Stucki *et al.* (1984c), however, postulated that the decrease in swelling was due to the conversion of fully expanded to unexpanded or partially expanded layers. Support was given to this postulate by the observation of Chen *et al.* (1987) that the reduction of octahedral Fe in clays enhanced their ability to fix K^+, i.e., to trap K^+ between their superimposed layers. A more direct test of the postulate, however, was needed. The purpose of the research described herein was to provide such a test.

MATERIALS AND METHODS

For the present study, a nontronite from Garfield, Washington (API #33) was selected as a model clay mineral having a relatively high iron content, namely, 4.2 mmole/g. The <2-μm size fraction of this nontronite was prepared in the Na-saturated, freeze-dried form, as described by Stucki *et al.* (1984c).

Suspensions of the nontronite were reduced to different degrees with sodium dithionite, as described by Stucki *et al.* (1984a), and dialyzed free of excess electrolyte against a 10^{-4} M solution of NaCl in the absence of oxygen, as described by Chen *et al.* (1987). Part of each reduced suspension was analyzed for Fe^{2+} and total Fe by the method of Stucki (1981). The rest of the suspension was used to determine the relation between the swelling pressure, Π, and the interlayer distance, λ, by an adaptation of the method of Viani *et al.* (1983). For this determination, a new type of environmental chamber had to be designed and constructed so that the reduced nontronite would not be exposed to the oxygen of the air during the determination. The chamber is illustrated in Figures 1a and 1b and is described below.

The new environmental chamber consisted of an anodized aluminum cylinder, a, containing passivated beryllium windows, b and b′, for the transmission of X-rays, a transparent plastic front wall, c, which allowed visual observation of the interior, and an anodized aluminum back wall, d. The beryllium windows were held in place by anodized aluminum collars to which they were sealed by epoxy resin. These collars

[1] Journal paper 11,660, Purdue University Agricultural Station.

[2] Permanent address: Institute of Soil Science, Academia Sinica, Nanking, People's Republic of China.

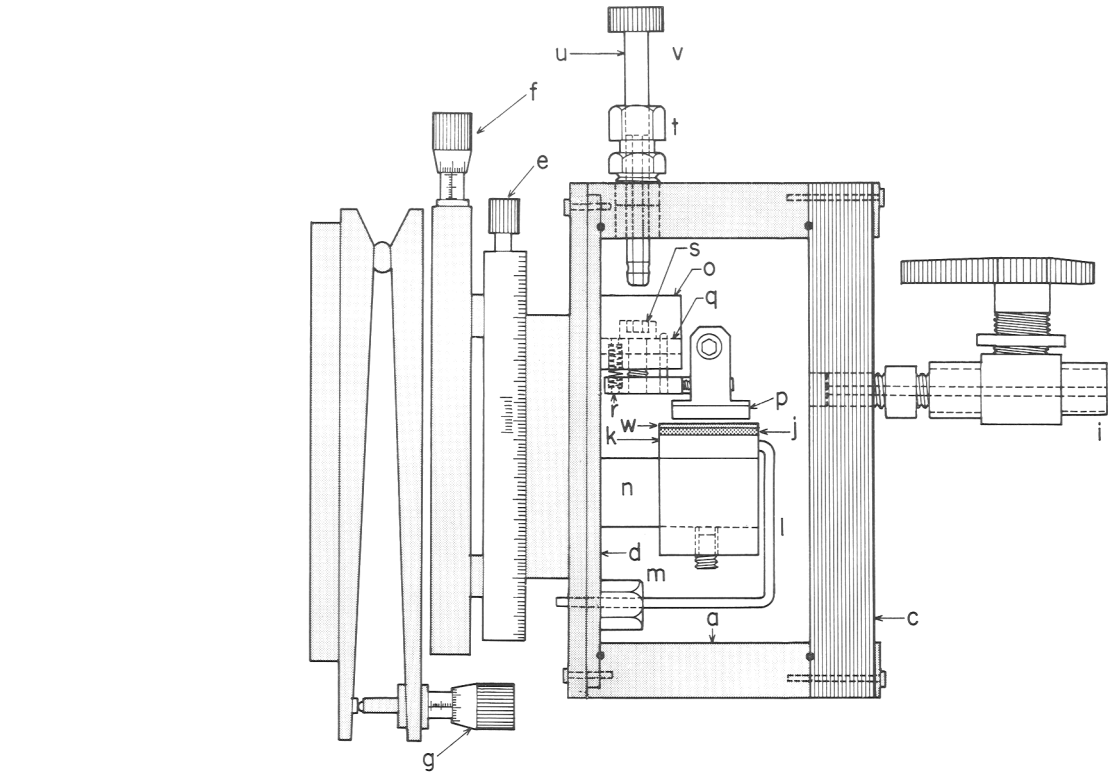

(a) Side View

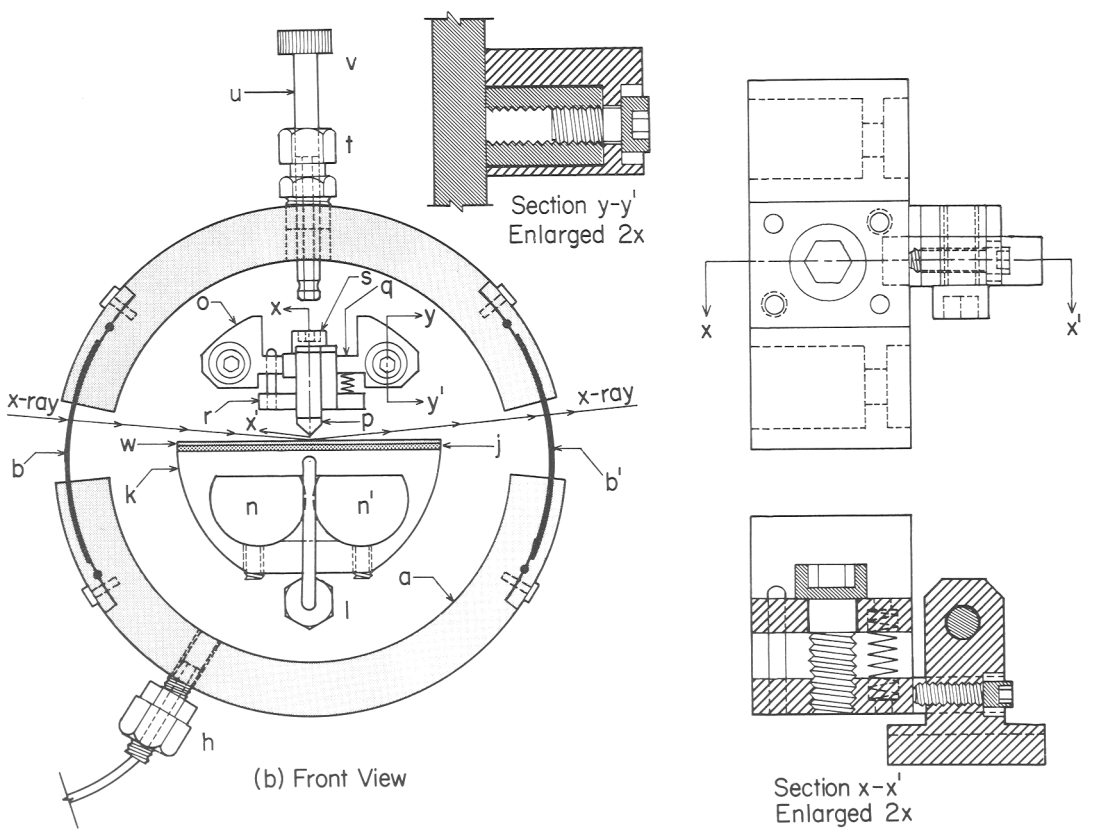

(b) Front View

Figure 1. (a) Cutaway side view of the environmental chamber. (b). Cutaway front view of the environmental chamber.

https://doi.org/10.1346/CCMN.1989.0370303 Published online by Cambridge University Press

and the front and back walls were separated from the cylinder by o-rings and were fastened to it by metal screws. Thus, leaks between the component parts were prevented. So that the chamber could be rotated, translated, or inclined (and, thereby, aligned on the focusing circle of the X-ray diffractometer), the back wall was attached to a series of stages controlled by the screws, e, f, and g. Two ports allowed gas to enter or leave the chamber. One of them, h, was connected through a pressure gauge and oxygen trap to a nitrogen (or helium) tank; the other was opened and closed by the ball valve, i.

At the center of the chamber was a device, commonly called a pressure plate or pressure membrane, in which a porous ceramic filter, j, with an air-entry pressure of ~15 atm, rested on the ridges between interconnected, parallel grooves in the bottom of a stainless steel reservoir, k, which was machined in the top of a solid metal support. The grooves were connected to the outside atmosphere by the drain tube, l, which passed through the pressure fitting, m. Leaks around the filter were prevented by sealing it to the wall of the reservoir with epoxy resin. The support under the reservoir was shaped to fit over two horizontal rods having flattened tops, n and n′, which projected from the back wall, d. Setscrews in the underside of the support could be tightened against these rods. Hence, the pressure membrane could be held stationary within the chamber or removed from it.

Located above the pressure membrane and secured to posts extending from the back wall by metal screws was a metal support, o, that was designed to allow the edge aperture, p, to be moved upwards or downwards above the porous ceramic filter. The primary components of the metal support were a fixed upper plate, q, a moveable lower plate, r, and a cap screw, s. The head of this screw was too large to pass through a hole in the upper plate; however, its shank passed through this hole and was screwed into the lower plate. The edge aperture was fastened to the latter plate. Alignment pins extended vertically from diagonally opposite corners of the lower plate, where they were anchored, through corresponding holes in the upper plate. Also, stiff spiral springs extended vertically between corresponding recesses in the other corners of the two plates. As a result, the plates were kept parallel and apart. To change the distance between them and, thereby, the level of the edge aperture, the cap screw could be turned clockwise or counterclockwise. This was accomplished by slightly loosening the pressure fitting, t, pushing the polished rod, u, downwards until its hexagonal tip engaged a similarly shaped indention in the top of the cap screw, and turning the knurled knob, v.

Before the environmental chamber was put into operation, and periodically thereafter, it was aligned on the X-ray goniometer in the following manner. A 1″ × 3″ glass slide coated with ZnS, an X-ray fluorescent material, was mounted in a special holder supported by the horizontal rods, n and n′, and the goniometer was advanced stepwise to approximately 10°2θ. Simultaneously, the chamber was translated and tilted with the screws f and g, respectively, until the image of the X-ray beam on the ZnS surface was symmetrical about the longitudinal axis of the slide. Then the goniometer was returned to 0°2θ, the 1″ × 3″ glass slide was replaced by two parallel glass slides held 0.002″ apart by spacers, and screws e and f were adjusted until the detector indicated a maximum in the intensity of the X-ray beam. During this operation, a copper filter was placed before the detector to keep it from being overloaded. Note that the glass slides formed a slit through which the X-ray beam had to pass and that the beam achieved its maximum intensity when the slit was coincident with it. Under this condition, the upper surface of the lower slide (and, hence, of any flat specimen in the same location) was tangential to the focusing circle of the diffractometer. Finally, to assure that proper alignment was achieved, the parallel glass slides were replaced successively by two different standards, namely, cholesterol (Kittrick, 1960) and novaculite (microcrystalline quartz) and, if the recorded diffractograms of these standards did not match the correct ones, the foregoing alignment process was repeated.

The procedure for using the environmental chamber was as follows:

1. After removing the appropriate screws and separating the cylinder from the back wall, the set screws and pressure fitting, m, were loosened, and the pressure membrane and its attachments were withdrawn from the supporting rods, n and n′.
2. To provide a retaining wall that was transparent to X-rays, a narrow strip of Mylar film was wrapped around the periphery of the filter and secured in place with plastic tape.
3. The pressure membrane and its attachments were evacuated in a desiccator.
4. A degassed, 10^{-4} M solution of NaCl was admitted, under vacuum, to the desiccator and allowed to saturate the filter and fill the underlying reservoir.
5. The solution-filled pressure membrane was quickly restored to its original position on the supporting rods, the setscrews and pressure fitting, m, were tightened, the cylinder was reinstalled on the back wall of the chamber, and the goniometer of the X-ray diffractometer was set at 0°2θ.
6. The chamber was flushed with oxygen-free nitrogen for about 30 min by opening the ball valve, i, and admitting nitrogen through the port, h.
7. A gas-tight syringe having a side-arm near the upper end of its barrel was flushed with oxygen-free nitrogen by admitting the nitrogen through the side-arm and letting it escape through the attached needle.

https://doi.org/10.1346/CCMN.1989.0370303 Published online by Cambridge University Press

8. A degassed, 10^{-4} M solution of NaCl was drawn into the barrel of the syringe.
9. The solution in the filter and reservoir was replaced two or three times by inserting the needle of the syringe through the ball valve, i, while nitrogen was escaping through it, dispensing fresh solution onto the filter, withdrawing the needle, and, after closing the ball valve, allowing a gauge presure of ~0.5 atm to develop.
10. After all the NaCl solution had been dispensed from the syringe, the reduced clay suspension was drawn into it, in the absence of air, by the procedure of Chen *et al.* (1987); the suspension was then deposited on the filter by the above procedure.
11. After the clay had formed an oriented gel, w, on the filter, the same procedure was used to add a few drops of a degassed suspension of silver-sheen mica (a synthetic, finely divided mica) or Na-kaolinite, which served as an internal standard.
12. With the ball valve, i, closed, the edge aperture was adjusted to its proper position, as described above, and water was expressed from the gel until equilibrium was reached under the pressure established by the nitrogen gas (or by oxygen-free helium which was often used, especially at higher pressures, to reduce attenuation of the X-rays).
13. Screw f was adjusted until the flat surface of the oriented clay gel was tangential to the focusing circle of the X-ray diffractometer (as indicated by the internal standard).
14. X-ray powder diffraction data were obtained with CuKα radiation using a 1° divergence slit and a ⅛° detector slit at intervals of 0.01° or 0.02°2θ over the 001 peak of the fully expanded layers and then at intervals of 0.04° thereafter out to 7°2θ.
15. The pressure of the gas in the chamber was raised and steps 12 through 14 were repeated.

The X-ray powder diffraction data were transmitted to a computer where they were smoothed, i.e., corrected point-by-point to agree with the polynomial describing the best-fitting curve through them, and corrected for the Lorentz-polarization (L_P) factor (Reynolds, 1976). The single-crystal version of this factor was used because of the high degree of orientation of the particles and the low angles of diffraction involved. The position of the 001 diffraction peak was then determined by processing the smoothed and L_P-corrected data by means of a computer program designed to locate the centroid of the peak. If this program could not be used because of interference from an adjacent peak, the same data were used to plot the diffractogram, and the peak was located visually. In either procedure, the result was corrected for any displacement error, indicated by the internal standard, before the corresponding *c*-axis spacing was calculated by Bragg's law. By subtracting the thickness of an individual clay layer (9.3 Å) from this spacing, λ was obtained. The maximum deviation from the mean value of λ decreased from <1.0 Å to <0.3 Å as λ decreased from ~50 Å to ~7.0 Å. At equilibrium, the swelling pressure, Π, of the clay equaled the applied pressure. Preliminary experiments showed no detectable changes in the X-ray powder diffraction patterns after 8–12-hr equilibration, and, hence, that equilibrium was achieved in this period of time. At least 18–24 hr, however, was allowed at each applied pressure before data were collected. Thus, we were able to obtain λ as a function of Π.

RESULTS AND DISCUSSION

If mica was used as an internal standard, the presence of fully collapsed layers in a smectite could not be detected because the 001 peaks of the mica and collapsed smectite layers are coincident. This was not true if kaolinite was used as an internal standard. Therefore, to determine whether or not the reduction of octahedral Fe in nontronite causes its superimposed layers to collapse fully, Na-kaolinite was used as an internal standard in some of the experiments. The results were negative. No peaks characteristic of fully collapsed layers were found. This does not necessarily mean that such layers were absent, but it does mean that they were not present in sufficient numbers to form X-ray diffracting domains. Note, however, that the nontronite was not dried following reduction. Had it been dried and rewetted, fully collapsed layers may have become evident.

Although the reduction of octahedral Fe in nontronite did not cause the mineral layers to collapse fully to any appreciable extent prior to drying, it did cause them to collapse partially or, in other words, to become partially expanded. This reaction is illustrated in Figures 2 and 3. Figure 2 applies if Π = 5 atm and Fe^{2+}/Fe^{3+} = 0.64 (Fe^{2+}/Fe_{total} = 0.39); whereas, Figure 3 applies if Π = 5 atm and Fe^{2+}/Fe^{3+} = 1.78 (Fe^{2+}/Fe_{total} = 0.64). Note that peaks corresponding to both fully expanded layers (2θ = 2.25°) and partially expanded layers (2θ = 4.53°) are evident in the former figure but only a single peak corresponding to partially expanded layers is evident in the latter.

X-ray powder diffraction patterns of the nontronite were obtained at several values of Π at each of several Fe^{2+}/Fe^{3+} ratios. The patterns corresponding to Fe^{2+}/Fe^{3+} ratios of 0.018, 0.64, and 1.78 are shown in Figures 4, 5, and 6, respectively. The first of these ratios is that of the non-reduced nontronite. In Figures 4 and 5, three peaks are evident, especially at low values of Π. Two of the peaks shifted progressively to higher values of 2θ with increasing Π and, at each value of Π, had locations indicating that they corresponded to the first- and second-order reflections from fully expanded layers. Also, at any given value of Π, their locations are the same in both illustrations. The third peak re-

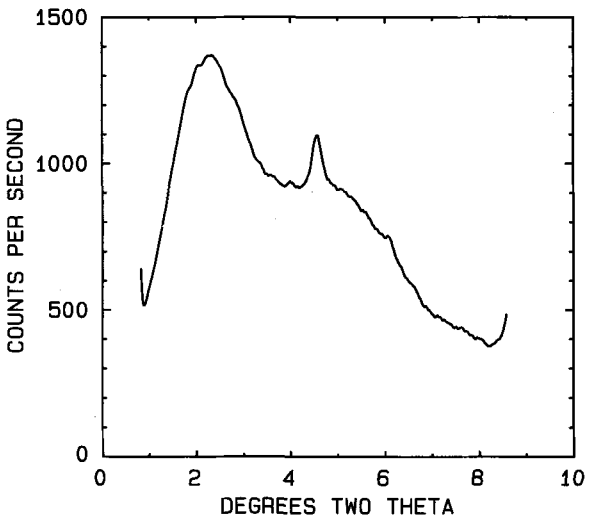

Figure 2. X-ray powder diffractogram of reduced Na-nontronite for Fe^{2+}/Fe^{3+} = 0.64 and swelling pressure = 5 atm (CuKα radiation).

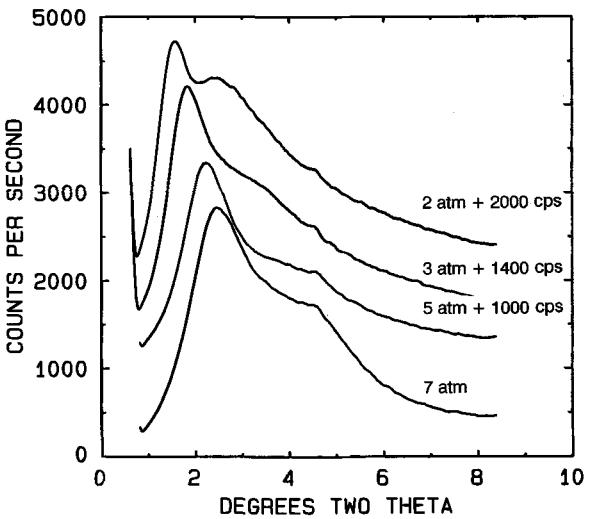

Figure 4. X-ray powder diffractograms of non-reduced Na-nontronite for Fe^{2+}/Fe^{3+} = 0.018 at different values of the swelling pressure (CuKα radiation).

mained stationary but increased in size with increasing II and had a location indicating that it corresponded to the first-order reflection from partially expanded layers. It is more prominent and has a slightly higher value of 2θ in Figure 5 than in Figure 4. Only a single peak is evident in Figure 6, however, and it remained essentially stationary with increasing II. This peak is broader, has a much greater intensity and occurs at a higher value of 2θ than the corresponding stationary peak in either of the preceding two illustrations. Although the relative intensities of the stationary peaks at different values of Fe^{2+}/Fe^{3+} are indicative of the relative numbers of diffracting layers, the relative breadths of these peaks are not necessarily indicative of the relative ranges over which λ is distributed. The breadth of the peaks is also influenced by the degree of orientation of the particles (stacks of layers), which depends on their degree of dispersion at the time of deposition. As reduction of octahedral Fe proceeded, the particles tended to become less dispersed. Therefore, the distance between the *fully expanded* layers must have depended on II but not on Fe^{2+}/Fe^{3+}, the distance between the *partially expanded* layers must have depended on Fe^{2+}/Fe^{3+} but not on II, and the

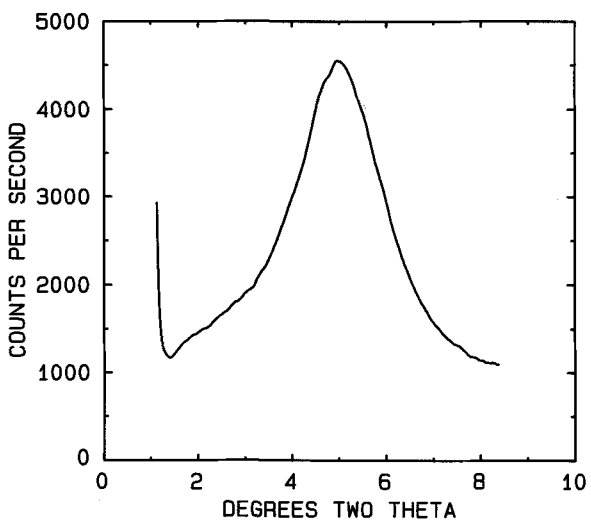

Figure 3. X-ray powder diffractogram of reduced Na-nontronite for Fe^{2+}/Fe^{3+} = 1.78 and swelling pressure = 5 atm (CuKα radiation).

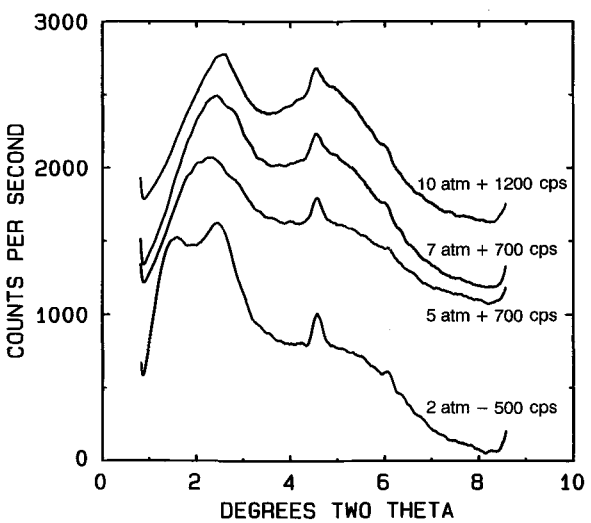

Figure 5. X-ray powder diffractograms of reduced Na-nontronite for Fe^{2+}/Fe^{3+} = 0.64 at different values of swelling pressure (CuKα radiation).

https://doi.org/10.1346/CCMN.1989.0370303 Published online by Cambridge University Press

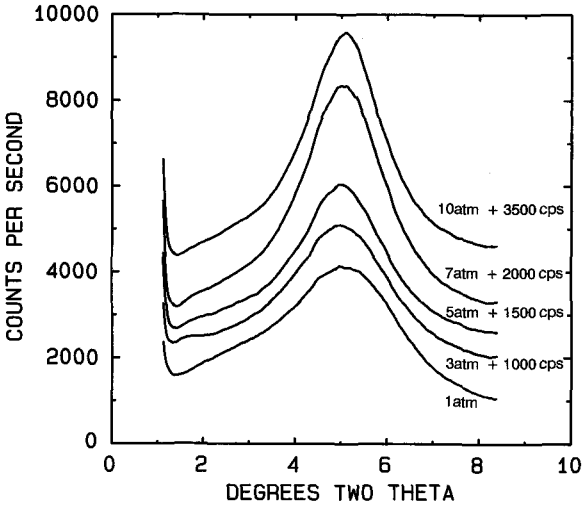

Figure 6. X-ray powder diffractograms of reduced Na-nontronite for Fe^{2+}/Fe^{3+} = 1.78 at different values of swelling pressure (CuKα radiation).

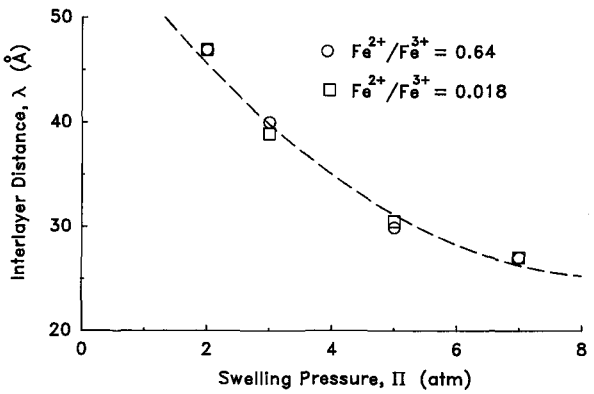

Figure 7. Relation between interlayer distance and swelling pressure for fully expanded layers of Na-nontronite at two different stages of reduction (dashed line represents lower limit of relations between interlayer distance and swelling pressure for Na-smectites and Li-vermiculite studied by Viani *et al.*, 1983, 1985).

fraction of partially expanded layers increased with both Π and Fe^{2+}/Fe^{3+}. These conclusions are reinforced by the data in Figures 7 and 8.

As shown in Figure 7, the relation between λ and Π for the fully expanded layers is the same for the partially reduced nontronite (Fe^{2+}/Fe^{3+} = 0.64) as for the non-reduced nontronite (Fe^{2+}/Fe^{3+} = 0.018). Three plausible explanations are possible for this observation. The first is that the reduction of octahedral Fe proceeded sequentially, layer by layer, and the fully expanded layers in the partially reduced clay were those that had not yet been reduced. The second is that the reduction of octahedral Fe proceeded randomly, but some of the layers contained no octahedral Fe and, hence, were unaffected by reduction. The third is that the reduction of octahedral Fe proceeded randomly in all layers and affected the short-range forces but not the long-range forces operating between the layers. As a result, reduction increased the proportion of partially expanded layers and decreased the distance between them, but did not affect the distance between the layers that remained fully expanded. If, however, the reduction of octahedral Fe proceeded sequentially and was finished in one layer before it began in the next, only one *c*-axis spacing should have existed for the partially expanded layers, namely, that characteristic of the highest Fe^{2+}/Fe^{3+} ratio attainable. Figure 8 shows that this was not the case. Further, if some of the layers contained no octahedral Fe, fully expanded layers should always have been present regardless of the degree of reduction. Figures 3 and 6 show that this was not so. We conclude, therefore, that the third explanation is the most plausible.

With respect to Figure 8, it should be noted that each value of λ reported therein is the average of values obtained at five different applied pressures ranging from 1 to 10 atm and that the standard deviation from the average is <0.3 Å, which is less than the width of a data point. Hence, λ for the partially expanded layers did not depend on Π; however, as indicated in the illustration, λ decreased with increasing Fe^{2+}/Fe^{3+}.

To account for these observations, we propose that: (1) the relations between ϵ, the mutual potential energy of the layers, and λ at different values of Fe^{2+}/Fe^{3+} can be represented qualitatively by the curves in Figure 9; (2) the partially expanded layers were in a primary energy minimum where they were subject to both short-range and long-range forces; (3) the fully expanded layers were beyond the energy barrier where they were subject to long-range forces only; and (4), the distribution of the layers between the partially expanded and fully expanded states was governed by the Maxwell-Boltzmann equation, viz.,

$$n_1/n_2 = e^{-(\epsilon_1-\epsilon_2)/kT} \quad (1)$$

where n_1 and n_2 are the numbers of layers in the partially expanded and fully expanded states, respectively, ϵ_1 and ϵ_2 are the corresponding energies of the layers in these states, k is the Boltzmann constant, and T is the absolute temperature.

Observe that Figure 9 has been drawn to show that the value of λ for the primary energy minimum decreases and the depth of this minimum increases as Fe^{2+}/Fe^{3+} increases, that the relation between ϵ and λ is independent of Fe^{2+}/Fe^{3+} for layers that are beyond the energy barrier, and that ϵ increases gradually with decreasing λ for these layers. Therefore, if our proposals are correct, the proportion of layers in the partially expanded state should have increased as Fe^{2+}/Fe^{3+} increased, i.e., as ϵ_1 became more negative, and as the fully expanded layers came closer together, i.e., as ϵ_2

https://doi.org/10.1346/CCMN.1989.0370303 Published online by Cambridge University Press

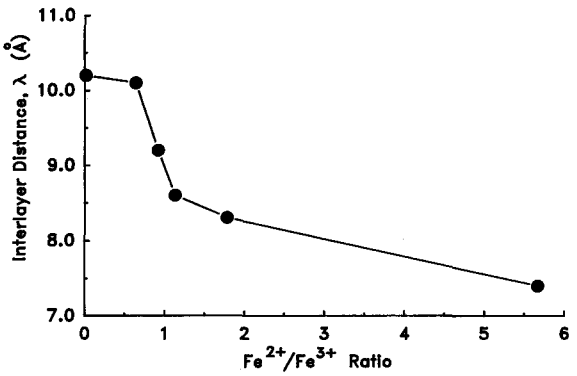

Figure 8. Relation between interlayer distance and Fe^{2+}/Fe^{3+} for partially expanded layers of Na-nontronite at all values of swelling pressure.

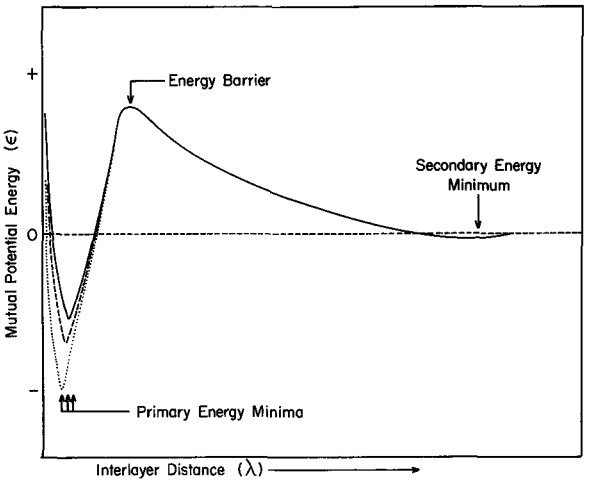

Figure 9. Proposed qualitative relations between mutual potential energy and interlayer distance of nontronite layers having different Fe^{2+}/Fe^{3+} ratios for octahedral iron (—— low Fe^{2+}/Fe^{3+}, – – – intermediate Fe^{2+}/Fe^{3+}, ····· high Fe^{2+}/Fe^{3+}).

became more positive. Moreover, the distance between the partially expanded layers should have decreased but the distance between the fully expanded layers should have remained unchanged as Fe^{2+}/Fe^{3+} increased. Further, an increase in pressure should have had little effect on the interlayer distance of the partially expanded layers (because of the narrowness of the energy minimum that they occupied), but should have decreased the interlayer distance of the fully expanded layers. All of these predictions are consistent with the experimental results.

The work of Viani *et al.* (1983, 1985) also supports the concept that changes in the chemistry of clay layers affect only the short-range forces between them, namely, the forces that do not extend beyond the energy barrier in Figure 9. They studied the relation between λ and Π for several expanding phyllosilicates (eight Na-smectites and Li-vermiculite) having a wide range of layer charge and found that the value of Π at which partially expanded layers became evident and that the value of λ for these layers decreased as the layer charge increased (e.g., λ was ~10 Å for the Na-smectites and ~6 Å for the Li-vermiculite). The relation between λ and Π for the fully expanded layers, however, was not affected by the layer charge. All of the curves of λ vs. Π for the fully expanded layers in the different clays fell between narrow limits. The lower of these limits is delineated by the dashed line in Figure 7. Note that the data points for the Na-nontronite are within experimental error of this line. In other words, the relation between λ and Π for the fully expanded layers in Na-nontronite is essentially the same as that for the fully expanded layers in all of the clays studied thus far. It appears, therefore, that the afore-mentioned concept is generally applicable.

Figure 7 also emphasizes the fact that layer charge has no significant effect on the long-range forces operating between fully expanded layers. Because the total Fe content of the nontronite was 4.2 mmole/g, the Fe^{2+} content of the partially reduced nontronite was 1.64 mmole/g and that of the non-reduced nontronite was 0.07 mmole/g. According to the data of Stucki *et al.* (1984b), the respective cation-exchange capacities are ~1.5 meq/g and ~1.0 meq/g. Therefore, the partial reduction of the nontronite increased its cation-exchange capacity (and, hence, its layer charge) by 50%. Yet the relation between λ and Π for the fully expanded layers remained unchanged.

Stucki *et al.* (1984c) observed that Π decreased with increasing Fe^{2+}/Fe^{3+} at any value of m_w/m_c, the mass ratio of water to clay, and that m_w/m_c decreased with increasing Fe^{2+}/Fe^{3+} at any value of Π. The decrease in m_w/m_c with increasing Fe^{2+}/Fe^{3+} was generally more rapid at low values of Fe^{2+}/Fe^{3+} than at high values. These observations can now be explained as follows. As octahedral Fe was reduced and Fe^{2+}/Fe^{3+} increased, an increasing fraction of the layers collapsed to the partially expanded state in which the interlayer distance depended slightly on Fe^{2+}/Fe^{3+} but was independent of Π. Thus, if m_w/m_c (and, hence, the volume of the system) was kept constant, the layers that were capable of full expansion moved apart to occupy the volume occupied formerly by the layers that collapsed, and Π decreased accordingly. On the other hand, if Π was kept constant, the layers that were capable of full expansion were not able to move apart and remain there indefinitely because, at equilibrium, they must be separated by the distance that separated them initially, i.e., by the interlayer distance characteristic of the given value of Π. The net result was that the excess water was expelled from the system, and m_w/m_c decreased accordingly. Moreover, because most of the layers partially collapsed before Fe^{2+}/Fe^{3+} was equal to 1.78 (Figure 6) and because much higher values of Fe^{2+}/Fe^{3+} were attainable (Figure 8), the rate of change of

https://doi.org/10.1346/CCMN.1989.0370303 Published online by Cambridge University Press

m_w/m_c with Fe^{2+}/Fe^{3+} was evidently greatest at relatively low values of Fe^{2+}/Fe^{3+}. Once all the layers were in the partially collapsed state at a specific value of II, further decrease in m_w/m_c with increasing Fe^{2+}/Fe^{3+} must have been due to the slight changes in λ indicated in Figure 8.

As noted above, Chen *et al.* (1987) found that the reduction of octahedral Fe in clays enhanced their ability to fix K^+. To account for this observation, they postulated that a collapse or partial collapse of the layers accompanied the conversion of octahedral Fe^{3+} to Fe^{2+} and caused the entrapment of interlayer K^+. Note that K^+ fixation was measured after the clays had been dried. It now appears that their postulate was valid and that the layers that partially collapsed on octahedral Fe reduction tended to remain collapsed after drying and rewetting. Thus, K^+ fixation was enhanced.

In the present experiments with nontronite, a strong chemical reducing agent (sodium dithionite) was used to reduce the octahedral Fe. Stucki *et al.* (1987) and Wu *et al.* (1988), however, showed that bacteria are able to reduce octahedral Fe in clays. Further, Wu *et al.* (1988) showed that bacterial reduction is almost as effective as that produced by sodium dithionite and causes layer collapse. Therefore, the present results probably apply under natural as well as laboratory conditions. These results also have ramifications beyond the phenomena of swelling and K^+ fixation. Because reducing conditions often prevail in buried sediments and surface soils, the resulting reduction of octahedral Fe and layer collapse could affect diagenesis in the former and weathering in the latter. It could also affect certain industrial processes. For example, to beneficiate bentonite for the drilling industry, it is a common practice to spread the freshly-mined, blue-gray material on the surface of the ground and to let it remain there for several months. Undoubtedly, this practice results in the oxidation of octahedral Fe in the bentonite and the subsequent expansion of its partially collapsed layers. In other words, it yields a more highly dispersed bentonite having better rheological properties. Therefore, whenever conditions may be expected to influence the oxidation state of iron-bearing clays, due attention should be paid to the effect of these conditions on the physical behavior of the clays.

ACKNOWLEDGMENTS

The authors thank the U.S. Army Research Office (Grant No. DAAG29-84-K-0167, Subcontract No. 84-132) for financial support of this work. They also gratefully acknowledge the valuable contributions made by R. L. Hutchinson to the design, construction, testing, and preliminary application of the new environmental chamber.

REFERENCES

Chen, S. Z., Low, P. F., and Roth, C. B. (1987) Relation between potassium fixation and oxidation state of octahedral iron: *Soil Sci. Soc. Amer. J.* **51,** 82–86.

Foster, M. D. (1953) Geochemical studies of clay minerals: II. Relation between ionic substitution and swelling in montmorillonites: *Amer. Mineral.* **38,** 994–1006.

Foster, W. R., Savins, J. G., and Waite, J. M. (1955) Lattice expansion and rheological behavior relationships in water-montmorillonite systems: in *Clays and Clay Minerals, Proc. 3rd Natl. Conf., Houston, Texas, 1954,* W. O. Milligan, ed., *Natl. Acad. Sci.-Natl. Res. Counc. Publ.* **395,** Washington, D.C., 296–316.

Kittrick, J. A. (1960) Cholesterol as a standard in the X-ray diffraction of clay minerals: *Soil Sci. Soc. Amer. Proc.* **24,** 17–20.

Kohyama, N., Shimoda, S., and Sudo, T. (1973) Iron-rich saponite (ferrous and ferric forms): *Clays & Clay Minerals* **21,** 229–237.

Ravina, I. and Low, P. F. (1972) Relation between swelling, water properties and *b*-dimension in montmorillonite-water systems: *Clays & Clay Minerals* **20,** 109–123.

Ravina, I. and Low, P. F. (1977) Change of *b*-dimension with swelling of montmorillonite: *Clays & Clay Minerals* **25,** 196–200.

Reynolds, R. C. (1976) The Lorentz factor for basal reflections from micaceous minerals in oriented powder aggregates: *Amer. Mineral.* **61,** 484–491.

Rhoades, J. D., Ingvalson, R. D., and Stumpf, H. T. (1969) Interlayer spacing of expanded clay minerals at various swelling pressures: An X-ray diffraction technique for direct determination: *Soil Sci. Soc. Amer. Proc.* **33,** 473–475.

Stucki, J. W. (1981) The quantitative assay of minerals for Fe^{2+} and Fe^{3+} using 1,10-phenanthroline. II. A photochemical method: *Soil Sci. Soc. Amer. J.* **45,** 638–641.

Stucki, J. W., Golden, D. C., and Roth, C. B. (1984a) Preparation and handling of dithionite-reduced smectite suspensions: *Clays & Clay Minerals* **32,** 191–197.

Stucki, J. W., Golden, D. C., and Roth, C. B. (1984b) Effects of reduction and reoxidation of structural iron on the surface charge and dissolution of dioctahedral smectites: *Clays & Clay Minerals* **32,** 350–356.

Stucki, J. W., Low, P. F., Roth, C. B., and Golden, D. C. (1984c) Effects of oxidation state of octahedral iron on clay swelling: *Clays & Clay Minerals* **32,** 357–362.

Stucki, J. W., Komadel, P., and Wilkinson, H. T. (1987) Microbial reduction of structural iron(III) in smectites: *Soil Sci. Soc. Amer. J.* **51,** 1663–1665.

Viani, B. V., Low, P. F., and Roth, C. B. (1983) Direct measurement of the relation between interlayer force and interlayer distance in the swelling of montmorillonite: *J. Colloid Interface Sci.* **96,** 229–244.

Viani, B. V., Roth, C. B., and Low, P. F. (1985) Direct measurement of the relation between swelling pressure and interlayer distance in Li-vermiculite: *Clays & Clay Minerals* **33,** 244–250.

Wu, J., Roth, C. B., and Low, P. F. (1988) Biological reduction of structural iron in Na-nontronite: *Soil Sci. Soc. Amer. J.* **52,** 295–296.

(Received 25 April 1988; accepted 30 September 1988; Ms. 1780)